AIAA JOURNAL
Vol. 47, No. 12, December 2009

Efficient Laminate Theory for Predicting Transverse Shear Stresses in Piezoelectric Composite Plates

S. Kapuria* and J. K. Nath†
Indian Institute of Technology-Delhi, New Delhi 110 016, India

DOI: 10.2514/1.44529

A new coupled efficient layerwise higher-order theory is presented for analysis of hybrid piezoelectric composite plates with the aim of predicting transverse shear stresses directly from the constitutive equations. The theory is developed by superposing layerwise quadratic and cubic terms on the third-order zigzag approximations of the existing zigzag theory. The electric potential is assumed to be quadratic across the layers. By satisfying the interface continuity conditions for each of the two local terms separately and enforcing the conditions on the transverse shear stresses at layer interfaces and top and bottom surfaces, the number of displacement unknowns is reduced to nine. Comparisons with the three-dimensional exact solutions reveal that the present theory is a significant improvement over the existing zigzag theory for elastic and hybrid composite plates. It yields superior results, not only for transverse shear stresses, but also for other response entities, including the layerwise higher-order variations of in-plane displacements and nonuniform distribution of deflection under electric potential load.

I. Introduction

LAMINATED composite plates are extensively used as structural members in aerospace, automotive, and shipbuilding industries today. Interlaminar transverse stresses are the predominant cause of failure (through delamination) in these laminated structures. In recent times, distributed piezoelectric sensors and actuators are integrated in these laminates to render self-sensing and actuation capabilities for active vibration control, shape control, noise control, and health monitoring (sensing) applications. In most cases, these piezoelectric elements are poled parallel to the applied electric field (in the thickness direction) and the membrane strains induced in them by the applied electric potential are used for the actuation (and conversely sensing), which is known as the extension actuation mechanism. This, however, induces large interlaminar transverse shear stresses at the interface between the actuated piezoelectric layer and the elastic laminate called the substrate, which may lead to weakening/delamination at the interface, causing drastic reduction in the actuating/sensing authority of the piezoelectric layer despite potential structural failure. The accurate prediction of interlaminar transverse stresses in elastic and piezoelectric laminates through a two-dimensional (2-D) laminate theory that is efficient, directly using constitutive equations, is a challenging task before the researchers. The present work is aimed to address this important issue.

A recent review of the state-of-the-art of smart structures can be found in [1]. Analytical three-dimensional (3-D) piezoelasticity solutions yield an accurate prediction of the interlaminar stresses in piezoelectric laminated structures, but such solutions are available only for some specific geometries and boundary conditions [2–4]. Among the available 2-D theories for hybrid plates, the coupled discrete layer theories (DLTs) [5] considering layerwise linear variation of displacements and electric potential are the most accurate, but they suffer from an excessive number of displacement unknowns in proportion to the number of layers. Moreover, the DLTs with layerwise linear variation yield constant shear stresses through each layer and hence require a large number of discrete layers to obtain the accurate profiles of transverse shear stresses across the thickness. Coupled first-order shear deformation theory (FSDT) [6–8], refined third-order theory (TOT) [9,10], and consistent TOT [11] have been developed, wherein the displacements are assumed to follow a global (first and higher order) variation across the thickness. These theories violate the slope discontinuity of in-plane displacements and the continuity of transverse shear stresses at the layer interfaces, yielding inaccurate global (deflection, in-plane stresses, etc.) as well as local (transverse stresses) response of moderately thick and even thinner laminates. Kapuria [12] and Kapuria and Achary [13] extended the efficient zigzag theory (ZIGT) of elastic laminated plates [14,15] to the fully coupled electromechanical response of hybrid piezoelectric plates, wherein the assumptions of displacements are the same as in the DLTs with additional quadratic and cubic global variation across thickness for the in-plane displacements and, incorporating nonuniform variation of transverse displacement, contributed by the electric field. But the number of displacement variables is reduced to only five, like FSDT and TOT, by enforcing transverse shear continuity conditions at layer interfaces and shear traction free conditions at top and bottom surfaces exactly. This theory has been found to yield very accurate results for global static and dynamic response of hybrid plates with highly inhomogeneous composite as well as sandwich substrates. But, it is unable to accurately predict the transverse shear stresses directly from the constitutive equations, which can only be obtained by integrating the 3-D equations of momentum. The integration, however, requires computation of higher-order derivatives of displacements, which poses difficulties in the finite element implementation and is still a great concern. This issue was apparently first addressed for elastic laminated plates by Li and Liu [16], who proposed a global–local theory (GLT) wherein local layerwise terms up to the third order are combined with the global third-order variations of in-plane displacements using double-superposition hypothesis. The continuity of the local displacement terms at the layer interfaces is satisfied in two groups, and conditions on the transverse shear stresses are satisfied to reduce the number of unknown displacement variables to 11. The theory was shown to predict the transverse stresses accurately from constitutive equations without using any postprocessing method. The theory was later generalized for the mth-order global variation by Zhen and Wanji [17].

In the present work, a new fully coupled efficient layerwise higher-order theory is developed for hybrid plates by adding local second- and third-order terms to the ZIGT approximations [12,13] of in-plane displacements, with the aim of predicting transverse shear stresses directly from constitutive equations. By satisfying the continuity of

Received 23 March 2009; revision received 30 June 2009; accepted for publication 30 June 2009.

*Professor, Department of Applied Mechanics; kapuria@am.iitd.ac.in (Corresponding Author).
†Research Scholar, Department of Applied Mechanics.

in-plane displacements at layer interfaces for each of the local terms separately and enforcing the conditions on transverse shear stresses, the number of primary displacement variables is reduced to nine. The electric potential is assumed to follow a quadratic variation across the piezoelectric layers, unlike the piecewise linear variation assumed in [12,13]. The accuracy of the theory is assessed in comparison with the 3-D exact piezoelasticity solutions [4,18] for both elastic and hybrid simply supported rectangular composite plates. The new theory differs from the ZIGT [12], not only due to the inclusion of layerwise higher-order terms in the expansion of in-plane displacements and the higher-order variation of electric potential, but also due to the adoption of a more general approach in obtaining the final variations of displacements. The additional displacement and potential variables lead to additional equations of momentum and charge balance. Most important, the new theory yields quite an accurate prediction of transverse shear stresses in elastic as well as hybrid laminates, which the earlier ZIGT and other theories of the same efficiency are unable to do.

II. Displacement and Electric Field Approximations

Consider a hybrid piezoelectric rectangular plate (Fig. 1) of thickness h consisting of L perfectly bonded orthotropic layers with the midplane chosen as the x–y plane. The plate is loaded transversely on its top and bottom surfaces. Some of its layers are of orthorhombic piezoelectric material exhibiting class mm2 symmetry [19] with poling along the thickness direction z. The z coordinate of the bottom surface of the kth layer from the bottom is denoted as $z = z_{k-1}$. The layer in which the reference plane lies, or is at the bottom of, is denoted as the k_0th layer.

Using the usual assumption of negligible transverse normal stress [$\sigma_z(\sigma_z \simeq 0)$] made in most 2-D theories, the 3-D linear constitutive equations of piezoelasticity [19,20] reduce to

$$\sigma = \bar{Q}\varepsilon - \bar{e}_3^T E_z, \qquad \tau = \hat{Q}\gamma - \hat{e}E$$
$$D = \hat{e}^T\gamma + \hat{\eta}E, \qquad D_z = \bar{e}_3\varepsilon + \bar{\eta}_{33}E_z \tag{1}$$

where

$$\sigma = \begin{bmatrix} \sigma_x \\ \sigma_y \\ \tau_{xy} \end{bmatrix}, \quad \tau = \begin{bmatrix} \tau_{zx} \\ \tau_{yz} \end{bmatrix}, \quad D = \begin{bmatrix} D_x \\ D_y \end{bmatrix}$$

$$\varepsilon = \begin{bmatrix} \varepsilon_x \\ \varepsilon_y \\ \gamma_{xy} \end{bmatrix}, \quad \gamma = \begin{bmatrix} \gamma_{zx} \\ \gamma_{yz} \end{bmatrix}, \quad E = \begin{bmatrix} E_x \\ E_y \end{bmatrix}$$

$$\bar{Q} = \begin{bmatrix} \bar{Q}_{11} & \bar{Q}_{12} & \bar{Q}_{16} \\ \bar{Q}_{12} & \bar{Q}_{22} & \bar{Q}_{26} \\ \bar{Q}_{16} & \bar{Q}_{26} & \bar{Q}_{66} \end{bmatrix}, \quad \hat{Q} = \begin{bmatrix} \bar{Q}_{55} & \bar{Q}_{45} \\ \bar{Q}_{45} & \bar{Q}_{44} \end{bmatrix}, \quad \hat{e} = \begin{bmatrix} \bar{e}_{15} & \bar{e}_{25} \\ \bar{e}_{14} & \bar{e}_{24} \end{bmatrix}$$

$$\hat{\eta} = \begin{bmatrix} \bar{\eta}_{11} & \bar{\eta}_{12} \\ \bar{\eta}_{12} & \bar{\eta}_{22} \end{bmatrix}, \quad \bar{e}_3 = [\bar{e}_{31} \;\; \bar{e}_{32} \;\; \bar{e}_{36}] \tag{2}$$

σ and ε are the in-plane stress and strain components, respectively; τ and γ denote the transverse shearing stress and strain components, respectively; $\bar{Q}_{ij}$, $\bar{e}_{ij}$, and $\bar{\eta}_{ij}$ are the reduced elastic stiffnesses, piezoelectric stress constants, and electric permittivities, respectively; and E_i and D_i ($i = x$, y, and z) denote the electric field and electric displacement components, respectively.

Let u_x, u_y, and w be the in-plane and transverse displacements and ϕ be the electric potential. The strain-displacement and electric field-electric potential relations for a small strain condition are

$$\varepsilon_x = u_{x,x}, \qquad \varepsilon_y = u_{y,y}, \qquad \varepsilon_z = w_{,z}$$
$$\gamma_{yz} = u_{y,z} + w_{,y}, \qquad \gamma_{zx} = u_{x,z} + w_{,x} \qquad \gamma_{xy} = u_{x,y} + u_{y,x}$$
$$E_x = -\phi_{,x}, \qquad E_y = -\phi_{,y}, \qquad E_z = -\phi_{,z} \tag{3}$$

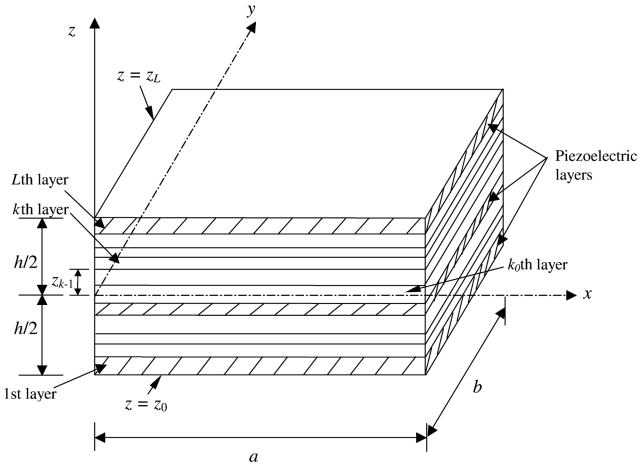

Fig. 1 Geometry of a hybrid plate.

The subscript comma denotes differentiation. The in-plane electric fields E_x and E_y may be applied by actuation through segmented piezoelectric actuator layers and/or induced due to the direct piezoelectric effect.

The 3-D piezoelasticity solutions [2–4] of piezoelectric plates poled along the thickness direction have shown that the electric potential ϕ in a piezoelectric layer follows a nearly quadratic distribution along the thickness. Accordingly, ϕ is approximated as a piecewise quadratic between n_ϕ points at $z = z_\phi^j$ across the thickness of the laminate:

$$\phi(x, y, z) = \Psi_\phi^j(z)\phi^j(x, y) + \Psi_c^q(z)\phi_c^q(x, y) \tag{4}$$

where $\phi^j(x, y) = \phi(x, y, z_\phi^j)$ denotes the electric potentials at piezoelectric layer surfaces/interfaces and $\phi_c^q(x, y)$ denotes the quadratic component of electric potential at $z = (z_\phi^q + z_\phi^{q+1})/2$. The summation convention is used for repeated indices, with the indices j and q taking values $j = 1, 2, \ldots, n_\phi$ and $q = 1, 2, \ldots, n_\phi - 1$. $\Psi_\phi^j(z)$ is a piecewise linear function and $\Psi_c^q(z)$ is a quadratic function given by

$$\Psi_\phi^j(z) = \begin{Bmatrix} 0 & \text{if } z \le z_\phi^{j-1} \text{ or } z \ge z_\phi^{j+1} \\ (z - z_\phi^{j-1})/(z_\phi^j - z_\phi^{j-1}) & \text{if } z_\phi^{j-1} < z < z_\phi^j \\ (z_\phi^{j+1} - z)/(z_\phi^{j+1} - z_\phi^j) & \text{if } z_\phi^j < z < z_\phi^{j+1} \end{Bmatrix}$$

$$\Psi_c^q(z) = \begin{Bmatrix} 4(z_\phi^{q+1} - z)(z - z_\phi^q)/(z_\phi^{q+1} - z_\phi^q)^2 & \text{if } z_\phi^q \le z \le z_\phi^{q+1} \\ 0 & \text{otherwise} \end{Bmatrix} \tag{5}$$

Exact 3-D piezoelasticity solutions [2–4] have also revealed that the thickness of a piezoelectric layer undergoes change primarily due to the d_{33} effect in presence of the electric field. To account for this transverse extensibility without introducing additional variables, the variation of deflection w is approximated by integrating the constitutive equation for ε_z by neglecting the contribution of elastic compliance and considering only the contribution of the electric field, as in [12]:

$$\varepsilon_z = w_{,z} \simeq -\bar{d}_{33}\phi_{,z}(z)$$
$$\Rightarrow w(x, y, z) = w_0(x, y) - \bar{\Psi}_\phi^j(z)\phi^j(x, y) - \bar{\Psi}_c^q(z)\phi_c^q(x, y) \tag{6}$$

where $\bar{\Psi}_\phi^j(z) = \int_0^z \bar{d}_{33}\Psi_{\phi,z}^j(z)\mathrm{d}z$ and $\bar{\Psi}_c^q(z) = \int_0^z \bar{\mathrm{d}}_{33}\Psi_{c,z}^q(z)\mathrm{d}z$. The in-plane displacements u_x and u_y are approximated by superposing local layerwise quadratic and cubic terms $\tilde{u}_L^k$ and $\hat{u}_L^k$ to the third-order zigzag variation of [12]:

$$u(x,y,z) = u_k(x,y) - zw_{0_d} + z\psi_k(x,y) + z^2\xi(x,y) + z^3\eta(x,y) + \bar{u}_L^k(x,y,\zeta_k) + \hat{u}_L^k(x,y,\zeta_k) \tag{7}$$

where

$$u = \begin{bmatrix} u_x \\ u_y \end{bmatrix}, \quad u_k = \begin{bmatrix} u_{k_x} \\ u_{k_y} \end{bmatrix}, \quad \psi_k = \begin{bmatrix} \psi_{k_x} \\ \psi_{k_y} \end{bmatrix}, \quad w_{0_d} = \begin{bmatrix} w_{0,x} \\ w_{0,y} \end{bmatrix}$$
$$\xi = \begin{bmatrix} \xi_x \\ \xi_y \end{bmatrix}, \quad \eta = \begin{bmatrix} \eta_x \\ \eta_y \end{bmatrix}, \quad \bar{u}_L^k = \begin{bmatrix} \bar{u}_{L_x}^k \\ \bar{u}_{L_y}^k \end{bmatrix}, \quad \hat{u}_L^k = \begin{bmatrix} \hat{u}_{L_x}^k \\ \hat{u}_{L_y}^k \end{bmatrix} \tag{8}$$

and the local terms $\bar{u}_L^k(x,y,\zeta_k)$ and $\hat{u}_L^k(x,y,\zeta_k)$ are given by

$$\bar{u}_L^k(x,y,\zeta_k) = \zeta_k^2 u_1^k(x,y), \qquad \hat{u}_L^k(x,y,\zeta_k) = \zeta_k^3 u_2^k(x,y) \tag{9}$$

with

$$u_1^k = \begin{bmatrix} u_{1_x}^k \\ u_{1_y}^k \end{bmatrix}, \quad u_2^k = \begin{bmatrix} u_{2_x}^k \\ u_{2_y}^k \end{bmatrix}, \quad \zeta_k = a_k z - b_k$$
$$a_k = \frac{2}{z_k - z_{k-1}}, \quad b_k = \frac{z_k + z_{k-1}}{z_k - z_{k-1}} \tag{10}$$

Similar to the double-superposition hypothesis of Li and Liu [16], the continuity of u at the layer interfaces is enforced separately for each of the local terms $\bar{u}_L^k$ and $\hat{u}_L^k$, and the group of remaining terms. This yields the following expressions for $\bar{u}_L^k$ and $\hat{u}_L^k$:

$$\begin{aligned} \bar{u}_L^k(z_k) = \bar{u}_L^{k+1}(z_k) &\Rightarrow \; u_1^k = u_1^0 \\ \hat{u}_L^k(z_k) = -\hat{u}_L^{k+1}(z_k) &\Rightarrow u_2^k = (-1)^k u_2^0 \end{aligned} \tag{11}$$

Substituting u_x and u_y from Eq. (7) in conjunction with Eqs. (9) and (11), and w from Eq. (6) into the strain-displacement relations for shear strains γ, and using the constitutive equation for τ from Eqs. (1), transverse shear stresses τ are obtained as

$$\tau = \hat{Q}^k[\psi_k + 2z\xi + 3z^2\eta + 2\zeta_k a_k u_1^0 + 3\zeta_k^2(-1)^k a_k u_2^0] + [\hat{e}^k\Psi_\phi^j(z) - \hat{Q}^k\bar{\Psi}_\phi^j(z)]\phi_d^j + [\hat{e}^k\Psi_c^q(z) - \hat{Q}^k\bar{\Psi}_c^q(z)]\phi_{c_d}^q \tag{12}$$

where

$$\phi_d^j = \begin{bmatrix} \phi_{,x}^j \\ \phi_{,y}^j \end{bmatrix}, \qquad \phi_{c_d}^q = \begin{bmatrix} \phi_{c,x}^q \\ \phi_{c,y}^q \end{bmatrix} \tag{13}$$

The conditions of zero transverse shear tractions on top and bottom surfaces and the continuity of τ and u at the layer interface between the ith and $(i+1)$th layers are imposed, which yields

$$\tau(z_0) = 0 \Rightarrow \psi_1 + 2z_0\xi + 3z_0^2\eta - 2a_1u_1^0 - 3a_1u_2^0 = \hat{Q}_{0j}\phi_d^j \tag{14}$$

$$\tau(z_i^-) = \tau(z_i^+) \Rightarrow \hat{Q}^{i+1}\psi_{i+1} - \hat{Q}^i\psi_i + 2z_i\hat{Q}_1^i\xi + 3z_i^2\hat{Q}_1^i\eta - 2\hat{Q}_2^iu_1^0 - 3(-1)^i\hat{Q}_2^iu_2^0 = \hat{Q}_{3j}^i\phi_d^j \tag{15}$$

$$\tau(z_L) = 0 \Rightarrow \psi_L + 2z_L\xi + 3z_L^2\eta + 2a_Lu_1^0 + 3a_L(-1)^Lu_2^0 = \hat{Q}_{Lj}\phi_d^j \tag{16}$$

$$u(z_i^-) = u(z_i^+) \Rightarrow u_{i+1} + z_i\psi_{i+1} - u_i - z_i\psi_i = 0 \tag{17}$$

where $i = 1, \ldots, L-1$; $\hat{Q}_1^i$, $\hat{Q}_2^i$, $\hat{Q}_{0j}$, $\hat{Q}_{Lj}$, and $\hat{Q}_{3j}^i$ are given by

$$\begin{aligned} \hat{Q}_1^i &= \hat{Q}^{i+1} - \hat{Q}^i, \qquad \hat{Q}_{0j} = \bar{\Psi}_\phi^j(z_0)I_2 - (\hat{Q}^1)^{-1}\hat{e}^1\Psi_\phi^j(z_0) \\ \hat{Q}_2^i &= \hat{Q}^{i+1}a_{i+1} + \hat{Q}^ia_i, \qquad \hat{Q}_{Lj} = \bar{\Psi}_\phi^j(z_L)I_2 - (\hat{Q}^L)^{-1}\hat{e}^L\Psi_\phi^j(z_L) \\ \hat{Q}_{3j}^i &= \hat{Q}_1^i\bar{\Psi}_\phi^j(z_i) + (\hat{e}^i - \hat{e}^{i+1})\Psi_\phi^j(z_i) \end{aligned} \tag{18}$$

and I_2 is a 2×2 identity matrix. Equations (14–17) can be written in the following matrix form for the $4L + 8$ unknowns u_k, ψ_k, u_1^0, u_2^0, ξ, and η:

$$A\bar{x} = B_j^\phi\phi_d^j \tag{19}$$

where A is a $4L \times (4L+8)$ matrix, B_j^ϕ is a $4L \times 2n_\phi$ matrix, and $\bar{x}$ is given by

$$\bar{x} = [\,u_1^T \quad \psi_1^T \quad u_2^T \quad \psi_2^T \quad \ldots \quad u_L^T \quad \psi_L^T \quad \xi^T \quad \eta^T \quad u_1^{0^T} \quad u_2^{0^T}\,]^T \tag{20}$$

The matrices A and B_j^ϕ are partitioned into 2×2 submatrices $A(p,q)$ and $B_j^\phi(p)$ and have the following nonzero submatrices:

$$\begin{aligned} A(1,2) &= I_2, & A(2i+1,2i) &= -z_iI_2 \\ A(1,2L+1) &= 2z_0I_2, & A(2i+1,2i+1) &= I_2 \\ A(1,2L+2) &= 3z_0^2I_2, & A(2i+1,2i+2) &= z_iI_2 \\ A(1,2L+3) &= -2a_1I_2, & A(2L,2L) &= I_2 \\ A(1,2L+4) &= -3a_1I_2, & A(2L,2L+1) &= 2z_LI_2 \\ A(2i,2i) &= -\hat{Q}^i, & A(2L,2L+2) &= 3z_L^2I_2 \\ A(2i,2i+2) &= \hat{Q}^{i+1}, & A(2L,2L+3) &= 2a_LI_2 \\ A(2i,2L+1) &= 2z_i\hat{Q}_1^i, & A(2L,2L+4) &= 3a_L(-1)^LI_2 \\ A(2i,2L+2) &= 3z_i^2\hat{Q}_1^i, & B_j^\phi(1) &= \hat{Q}_{0j} \\ A(2i,2L+3) &= -2\hat{Q}_2^i, & B_j^\phi(2i) &= \hat{Q}_{3j}^i \\ A(2i,2L+4) &= -3(-1)^i\hat{Q}_2^i, & B_j^\phi(2L) &= \hat{Q}_{Lj} \\ A(2i+1,2i-1) &= -I_2 \end{aligned} \tag{21}$$

for $i = 1, 2, \ldots, L-1$. Partitioning $\bar{x}$ into vectors of primary variables $\bar{x}_2$, corresponding to the reference surface and the remaining variables $\bar{x}_1$, $\bar{x}_1$ can be expressed in terms of $\bar{x}_2$ as

$$[A_1 \quad A_2]\begin{bmatrix} \bar{x}_1 \\ \bar{x}_2 \end{bmatrix} = B_j^\phi\phi_d^j \Rightarrow \bar{x}_1 = \bar{A}_2\bar{x}_2 + C_j^\phi\phi_d^j \tag{22}$$

where A_1 and A_2 are submatrices of size $4L \times 4L$ and $4L \times 8$, respectively, and

$$\begin{aligned} \bar{x}_1 &= [\,u_1^T \quad \psi_1^T \quad u_2^T \quad \psi_2^T \quad \ldots \quad u_i^T \quad \psi_i^T \quad \ldots \quad \xi^T \quad \eta^T\,]^T \\ &\quad i = 1, 2, \ldots, L \quad \text{and} \quad i \neq k_0 \\ \bar{x}_2 &= [\,u_0^T \quad \psi_0^T \quad u_1^{0^T} \quad u_2^{0^T}\,]^T \end{aligned} \tag{23}$$

$$\bar{A}_2 = -A_1^{-1}A_2, \qquad C_j^\phi = A_1^{-1}B_j^\phi \tag{24}$$

Let $\bar{A}_2^1$, $\bar{A}_2^2$, $\bar{A}_2^3$, and $\bar{A}_2^4$ be submatrices of matrix $\bar{A}_2$, each of size $4L \times 2$, such that

$$\bar{A}_2 = [\,\bar{A}_2^1 \quad \bar{A}_2^2 \quad \bar{A}_2^3 \quad \bar{A}_2^4\,] \tag{25}$$

Matrices $\bar{A}_2^i$ are further partitioned into 2×2 matrices $\bar{A}_2^i(p)$ for $p = 1, 2, \ldots, 2L$. Because ξ, η, and ψ_i in Eqs. (14–16) can be solved in terms of ψ_0, u_1^0, u_2^0, and ϕ_d^j, it follows that $\bar{A}_2^1(2i) = 0$ for $i = 1, \ldots, L$ and $\bar{A}_2^1(2L-1) = 0$. Also, Eq. (17) implies $u_i = u_0 + f(\psi_1, \psi_2, \ldots, \psi_L)$, where f is a function of ψ_i's. Thus $\bar{A}_2^1(2i-1) = I_2$ for $i = 1, 2, \ldots, L-1$. Using Eq. (22), the unknowns u_k, ψ_k, ξ, and η can be expressed explicitly as

$$
\begin{aligned}
u_k &= u_0 + \bar{A}_2^2(2k'-1)\psi_0 + \bar{A}_2^3(2k'-1)u_1^0 + \bar{A}_2^4(2k'-1)u_2^0 \\
&\quad + C_j^{\phi}(2k'-1)\phi_d^j \\
\psi_k &= \bar{A}_2^2(2k')\psi_0 + \bar{A}_2^3(2k')u_1^0 + \bar{A}_2^4(2k')u_2^0 + C_j^{\phi}(2k')\phi_d^j \\
\xi &= \bar{A}_2^2(2L-1)\psi_0 + \bar{A}_2^3(2L-1)u_1^0 + \bar{A}_2^4(2L-1)u_2^0 \\
&\quad + C_j^{\phi}(2L-1)\phi_d^j \\
\eta &= \bar{A}_2^2(2L)\psi_0 + \bar{A}_2^3(2L)u_1^0 + \bar{A}_2^4(2L)u_2^0 + C_j^{\phi}(2L)\phi_d^j
\end{aligned} \tag{26}
$$

with $k' = k$ for $k < k_0$ and $k' = k-1$ for $k > k_0$. Substituting the previous expressions of u_k, ψ_k, ξ, and η into Eq. (7) yields the final expression for u as

$$
\begin{aligned}
u(x,y,z) &= u_0 - zw_{0_d} + R^k(z)\psi_0 + \bar{R}^k(z)u_1^0 \\
&\quad + \hat{R}^k(z)u_2^0 + R^{kj}(z)\phi_d^j
\end{aligned} \tag{27}
$$

where $R^k(z)$, $\bar{R}^k(z)$, $\hat{R}^k(z)$, and $R^{kj}(z)$ are 2×2 matrices of functions of z, for which the expressions are given as follows.

For $k \neq k_0$,

$$
\begin{aligned}
R^k(z) &= \bar{A}_2^2(2k'-1) + z\bar{A}_2^2(2k') + z^2\bar{A}_2^2(2L-1) + z^3\bar{A}_2^2(2L) \\
\bar{R}^k(z) &= \bar{A}_2^3(2k'-1) + z\bar{A}_2^3(2k') + z^2\bar{A}_2^3(2L-1) \\
&\quad + z^3\bar{A}_2^3(2L) + \zeta_k^2 I_2 \\
\hat{R}^k(z) &= \bar{A}_2^4(2k'-1) + z\bar{A}_2^4(2k') + z^2\bar{A}_2^4(2L-1) \\
&\quad + z^3\bar{A}_2^4(2L) + \zeta_k^3(-1)^k I_2 \\
R^{kj}(z) &= C_j^{\phi}(2k'-1) + zC_j^{\phi}(2k') \\
&\quad + z^2C_j^{\phi}(2L-1) + z^3C_j^{\phi}(2L)
\end{aligned} \tag{28}
$$

For $k = k_0$,

$$
\begin{aligned}
R^k(z) &= zI_2 + z^2\bar{A}_2^2(2L-1) + z^3\bar{A}_2^2(2L) \\
\bar{R}^k(z) &= z^2\bar{A}_2^3(2L-1) + z^3\bar{A}_2^3(2L) + \zeta_k^2 I_2 \\
\hat{R}^k(z) &= z^2\bar{A}_2^4(2L-1) + z^3\bar{A}_2^4(2L) + \zeta_k^3(-1)^k I_2 \\
R^{kj}(z) &= z^2C_j^{\phi}(2L-1) + z^3C_j^{\phi}(2L)
\end{aligned} \tag{29}
$$

III. Coupled Equilibrium Equations and Boundary Conditions

The variational principle for the piezoelectric medium [20] can be expressed, using the notation

$$
\langle \ldots \rangle = \sum_{k=1}^{L} \int_{z_{k-1}^{+}}^{z_k^{-}} (\ldots)\mathrm{d}z
$$

for integration across the thickness, as

$$
\begin{aligned}
&\int_A [\langle \sigma_x\delta\varepsilon_x + \sigma_y\delta\varepsilon_y + \tau_{xy}\delta\gamma_{xy} + \tau_{yz}\delta\gamma_{yz} + \tau_{zx}\delta\gamma_{zx} + D_x\delta\phi_{,x} \\
&\quad + D_y\delta\phi_{,y} + D_z\delta\phi_{,z}\rangle - p_z^1\delta w(x,y,z_0) - p_z^2\delta w(x,y,z_L) \\
&\quad + D_z(x,y,z_0)\delta\phi^1 - D_z(x,y,z_L)\delta\phi^{n_\phi} - q_{j_i}\delta\phi^{j_i}]\mathrm{d}A \\
&\quad - \int_{\Gamma_L} \langle \sigma_n\delta u_n + \tau_{ns}\delta u_s + \tau_{nz}\delta w + D_n\delta\phi\rangle \mathrm{d}s = 0
\end{aligned} \tag{30}
$$

$\forall\ \delta u_0, \delta u_1^0, \delta u_2^0, \delta w_0, \delta\psi_0$, and $\delta\phi^j$. A is the midplane surface area of the plate and Γ_L is the boundary curve of the midplane, with normal $\underline{n}$ and tangent $\underline{s}$. p_z^1 and p_z^2 are the transverse loading per unit area on bottom and top surfaces, respectively. q_{j_i} denotes the jump in electric displacement D_z across the interface $z = z_\phi^{j_i}$, where ϕ^{j_i} is prescribed. The total number of such prescribed potentials is $\bar{n}_\phi$. This variational equation is expressed in terms of δu_0, δu_1^0, δu_2^0, δw_0, $\delta\psi_0$, and $\delta\phi^j$ to yield the governing equations and boundary conditions.

The stress resultants F_1 and F_2 and the electric displacement resultants F_3 and F_4 are defined by

$$
\begin{aligned}
F_1 &= [\,N^T \quad M^T \quad P^T \quad \bar{P}^T \quad \hat{P}^T \quad S^{j^T}\,]^T = [\langle f_3^T(z)\sigma\rangle] \\
F_2 &= [\,Q^T \quad \bar{Q}^T \quad \hat{Q}^T \quad \bar{Q}^{j^T} \quad \tilde{Q}^{q^T}\,]^T = [\langle f_4^T(z)\tau\rangle] \\
F_3 &= [\,H^{j^T} \quad \tilde{H}^{q^T}\,]^T = [\langle f_5^T(z)D\rangle] \\
F_4 &= [\,G^j \quad \tilde{G}^q\,]^T = [\langle f_6^T(z)D_z\rangle]
\end{aligned} \tag{31}
$$

with

$$
\begin{aligned}
N &= [\,N_x \quad N_y \quad N_{xy}\,]^T, & M &= [\,M_x \quad M_y \quad M_{xy}\,]^T \\
P &= [\,P_x \quad P_{yx} \quad P_{xy} \quad P_y\,]^T, & \bar{P} &= [\,\bar{P}_x \quad \bar{P}_{yx} \quad \bar{P}_{xy} \quad \bar{P}_y\,]^T \\
\hat{P} &= [\,\hat{P}_x \quad \hat{P}_{yx} \quad \hat{P}_{xy} \quad \hat{P}_y\,]^T, & S^j &= [\,S_x^j \quad S_{yx}^j \quad S_{xy}^j \quad S_y^j\,]^T \\
Q &= [\,Q_x \quad Q_y\,]^T, & \bar{Q} &= [\,\bar{Q}_x \quad \bar{Q}_y\,]^T \\
\hat{Q} &= [\,\hat{Q}_x \quad \hat{Q}_y\,]^T, & \bar{Q}^j &= [\,\bar{Q}_x^j \quad \bar{Q}_y^j\,]^T \\
\tilde{Q}^q &= [\,\tilde{Q}_x^q \quad \tilde{Q}_y^q\,]^T, & H^j &= [\,H_x^j \quad H_y^j\,]^T, & \tilde{H}^q &= [\,\tilde{H}_x^q \quad \tilde{H}_y^q\,]^T
\end{aligned} \tag{32}
$$

and

$$
\begin{aligned}
f_3(z) &= [\,I_3 \quad zI_3 \quad \Phi^k(z) \quad \bar{\Phi}^k(z) \quad \hat{\Phi}^k(z) \quad \Phi^{kj}(z)\,] \\
f_4(z) &= [\,R_{,z}^k(z) \quad \bar{R}_{,z}^k(z) \quad \hat{R}_{,z}^k(z) \quad R_{,z}^{kj}(z) - \bar{\Psi}_\phi^j(z)I_2 \quad -\bar{\Psi}_c^q I_2\,] \\
f_5(z) &= [\,\Psi^j(z)I_2 \quad \Psi_c^q(z)I_2\,], \qquad f_6(z) = [\,\Psi_{,z}^j(z) \quad \Psi_{c,z}^q(z)\,]
\end{aligned} \tag{33}
$$

$$
\begin{aligned}
\Phi^k &= \begin{bmatrix} R_{11}^k & 0 & R_{12}^k & 0 \\ 0 & R_{21}^k & 0 & R_{22}^k \\ R_{21}^k & R_{11}^k & R_{22}^k & R_{12}^k \end{bmatrix} \\
\bar{\Phi}^k &= \begin{bmatrix} \bar{R}_{11}^k & 0 & \bar{R}_{12}^k & 0 \\ 0 & \bar{R}_{21}^k & 0 & \bar{R}_{22}^k \\ \bar{R}_{21}^k & \bar{R}_{11}^k & \bar{R}_{22}^k & \bar{R}_{12}^k \end{bmatrix} \\
\hat{\Phi}^k &= \begin{bmatrix} \hat{R}_{11}^k & 0 & \hat{R}_{12}^k & 0 \\ 0 & \hat{R}_{21}^k & 0 & \hat{R}_{22}^k \\ \hat{R}_{21}^k & \hat{R}_{11}^k & \hat{R}_{22}^k & \hat{R}_{12}^k \end{bmatrix} \\
\Phi^{kj} &= \begin{bmatrix} R_{11}^{kj} & 0 & R_{12}^{kj} & 0 \\ 0 & R_{21}^{kj} & 0 & R_{22}^{kj} \\ R_{21}^{kj} & R_{11}^{kj} & R_{22}^{kj} & R_{12}^{kj} \end{bmatrix}
\end{aligned} \tag{34}
$$

where I_3 is a 3×3 identity matrix. The generalized stress resultants F_1, F_2, F_3, and F_4 can be expressed in terms of the displacement and potential variables by substituting the expressions of σ, τ, D, and D_z from Eqs. (1) into Eqs. (31) and using Eqs. (3), (4), (6), and (27):

$$
\begin{aligned}
F_1 &= A\bar{\varepsilon}_1 + \beta\bar{\varepsilon}_4, & F_2 &= \bar{A}\bar{\varepsilon}_2 + \bar{\beta}\bar{\varepsilon}_3 \\
F_3 &= \bar{\beta}^T\bar{\varepsilon}_2 - \bar{E}\bar{\varepsilon}_3, & F_4 &= \beta^T\bar{\varepsilon}_1 - \hat{E}\bar{\varepsilon}_4
\end{aligned} \tag{35}
$$

where

$$\bar{\varepsilon}_1 = [\,\varepsilon_0^T \quad K^T \quad \psi_{0_d}^T \quad u_{1_d}^{0^T} \quad u_{2_d}^{0^T} \quad \phi_{dd}^{j^T}\,]^T$$
$$\bar{\varepsilon}_2 = [\,\psi_0^T \quad u_1^{0^T} \quad u_2^{0^T} \quad \phi_d^{j^T} \quad \phi_{c_d}^{q^T}\,]^T$$
$$\bar{\varepsilon}_3 = [\,\phi_{,x}^j \quad \phi_{,y}^j \quad \phi_{c,x}^q \quad \phi_{c,y}^q\,]^T, \qquad \bar{\varepsilon}_4 = [\,\phi^j \quad \phi_c^q\,]^T$$
$$\varepsilon_0 = [\,u_{0_x,x} \quad u_{0_y,y} \quad u_{0_x,y} + u_{0_y,x}\,]^T$$
$$K = [\,-w_{0,xx} \quad -w_{0,yy} \quad -2w_{0,xy}\,]^T$$
$$\psi_{0_d} = [\,\psi_{0_x,x} \quad \psi_{0_x,y} \quad \psi_{0_y,x} \quad \psi_{0_y,y}\,]^T$$
$$u_{1_d}^0 = [\,u_{1_x,x}^0 \quad u_{1_x,y}^0 \quad u_{1_y,x}^0 \quad u_{1_y,y}^0\,]^T$$
$$u_{2_d}^0 = [\,u_{2_x,x}^0 \quad u_{2_x,y}^0 \quad u_{2_y,x}^0 \quad u_{2_y,y}^0\,]^T$$
$$\phi_{dd}^j = [\,\phi_{,xx}^j \quad \phi_{,xy}^j \quad \phi_{,yx}^j \quad \phi_{,yy}^j\,]^T$$
$$A = \langle f_3^T(z)\bar{Q}f_3(z)\rangle, \qquad \beta = \langle f_3^T(z)\bar{e}_3^T f_6(z)\rangle$$
$$\bar{A} = \langle f_4^T(z)\hat{Q}f_4(z)\rangle, \qquad \bar{\beta} = \langle f_4^T(z)\hat{e}f_5(z)\rangle$$
$$\bar{E} = \langle f_5^T(z)\hat{\eta}f_5(z)\rangle, \qquad \hat{E} = \langle f_6^T(z)\bar{\eta}_{33}f_6(z)\rangle \tag{36}$$

The area integral of Eq. (30) is expressed in terms of generalized virtual displacements δu_{0_x}, δu_{0_y}, δw_0, $\delta\psi_{0_x}$, $\delta\psi_{0_y}$, $\delta\phi^j$, and $\delta\phi_c^q$ by using the expressions of ϕ, w, and u from Eqs. (4), (6), and (27) and the definitions of generalized plate resultants in Eqs. (31), and by employing Green's theorem wherever required. Because the generalized virtual displacements are arbitrary, their coefficients are equalled to zero, resulting in the following equilibrium equations for the piezoelectric plate:

$$N_{x,x} + N_{xy,y} = 0, \qquad N_{xy,x} + N_{y,y} = 0$$
$$M_{x,xx} + 2M_{xy,xy} + M_{y,yy} + F_5 = 0, \qquad P_{x,x} + P_{yx,y} - Q_x = 0$$
$$P_{xy,x} + P_{y,y} - Q_y = 0, \qquad \bar{P}_{x,x} + \bar{P}_{yx,y} - \bar{Q}_x = 0$$
$$\bar{P}_{xy,x} + \bar{P}_{y,y} - \bar{Q}_y = 0, \qquad \hat{P}_{x,x} + \hat{P}_{yx,y} - \hat{Q}_x = 0$$
$$\hat{P}_{xy,x} + \hat{P}_{y,y} - \hat{Q}_y = 0, \qquad \tilde{Q}_{x,x}^q + \tilde{Q}_{y,y}^q + \tilde{H}_{x,x}^q + \tilde{H}_{y,y}^q - \tilde{G}^q = 0$$
$$S_{x,xx}^j + S_{xy,xy}^j + S_{yx,xy}^j + S_{y,yy}^j - \bar{Q}_{x,x}^j - \bar{Q}_{y,y}^j - H_{x,x}^j - H_{y,y}^j + G^j - F_6^j = 0 \tag{37}$$

for $j = 1, 2, \ldots, n_\phi$ and $q = 1, 2, \ldots, n_\phi - 1$. The mechanical load F_5 and the electrical loads F_6^j are defined as

$$F_5 = p_z^1 + p_z^2$$
$$F_6^j = -p_z^1\bar{\Psi}_\phi^j(z_0) - p_z^2\bar{\Psi}_\phi^j(z_L) + D_{z_L}\delta_{jn_\phi} - D_{z_0}\delta_{j1} + q_{j_i}\delta_{jj_i} \tag{38}$$

and δ_{ij} is Kronecker's delta. The terms involving components of virtual displacements in x and y directions in the integral of Γ_L are expressed in terms of components in $\underline{n}$ and $\underline{s}$ directions. This yields the following boundary conditions on Γ_L, where one of the factors of each of the following products are prescribed:

$$u_{0_n}N_n, \qquad u_{0_s}N_{ns}, \qquad w_0(V_n + M_{ns,s}), \qquad w_{0,n}M_n$$
$$\psi_{0_n}P_n, \qquad \psi_{0_s}P_{ns}, \qquad u_{1_n}^0\bar{P}_n, \qquad u_{1_s}^0\bar{P}_{ns}, \qquad u_{2_n}^0\hat{P}_n$$
$$u_{2_s}^0\hat{P}_{ns}, \qquad \phi^j(H^j - V_{\phi_n}^j - S_{ns,s}^j), \qquad \phi_{,n}^j S_n^j, \qquad \phi_c^q(\tilde{H}_n^q - \tilde{V}_{\phi_n}^q)$$

and at corners s_i

$$w_0(s_i)\Delta M_{ns}(s_i), \qquad \phi^j(s_i)\Delta S_{ns}^j(s_i) \tag{39}$$

where V_n, $V_{\phi_n}^j$, and $\tilde{V}_{\phi_n}^q$ are the mechanical and electromechanical resultants of transverse shear stresses given by $V_n = \langle\tau_{nz}\rangle$, $V_{\phi_n}^j = \langle\bar{\Psi}_\phi^j(z)\tau_{nz}\rangle$, and $\tilde{V}_{\phi_n}^q = \langle\bar{\Psi}_c^q(z)\tau_{nz}\rangle$.

Substituting the expressions of resultants from Eqs. (35) into Eqs. (37) yields the governing equations of equilibrium in terms of the primary displacements and electric potential variables in the following form:

$$L\bar{U} = \bar{P} \tag{40}$$

where

$$\bar{U} = [\,u_{0_x} \quad u_{0_y} \quad w_0 \quad \psi_{0_x} \quad \psi_{0_y} \quad u_{1_x}^0 \quad u_{1_y}^0 \quad u_{2_x}^0 \quad u_{2_y}^0 \quad \phi^1 \quad \phi^2 \quad \ldots \quad \phi^{n_\phi} \quad \phi_c^1 \quad \phi_c^2 \quad \ldots \quad \phi_c^{n_\phi - 1}\,]^T$$
$$\bar{P} = [\,0 \quad 0 \quad -F_5 \quad 0 \quad 0 \quad 0 \quad 0 \quad 0 \quad 0 \quad -F_6^1 \quad -F_6^2 \quad \cdots \quad -F_6^{n_\phi} \quad 0 \quad 0 \quad \cdots \quad 0\,]^T \tag{41}$$

L is a symmetric matrix of linear differential operators in x and y. For cross-ply plates, $\bar{Q}_{45} = 0$, $\bar{Q}_{16} = \bar{Q}_{26} = 0$, $\bar{e}_{14} = \bar{e}_{25} = 0$, $\bar{\eta}_{12} = 0$, and $\bar{e}_{36} = 0$.

To assess the accuracy of this theory, by comparison with the exact 3-D piezoelasticity solution [2,4], an analytical Navier solution is obtained for simply supported rectangular plate of sides a and b along the axes x and y for the following boundary conditions:

$$\text{at } x = 0, \qquad a\text{: } N_x = 0, \qquad u_{0_y} = 0, \qquad w_0 = 0, \qquad M_x = 0$$
$$P_x = 0, \qquad \psi_{0_y} = 0, \qquad \bar{P}_x = 0, \qquad u_{1_y}^0 = 0, \qquad \hat{P}_x = 0$$
$$u_{2_y}^0 = 0, \qquad \phi^j = 0, \qquad S_x^j = 0, \qquad \phi_c^q = 0$$
$$\text{at } y = 0, \qquad b\text{: } N_y = 0, \qquad u_{0_x} = 0, \qquad w_0 = 0, \qquad M_y = 0$$
$$P_y = 0, \qquad \psi_{0_x} = 0, \qquad \bar{P}_y = 0, \qquad u_{1_x}^0 = 0, \qquad \hat{P}_y = 0$$
$$u_{2_x}^0 = 0, \qquad \phi^j = 0, \qquad S_y^j = 0, \qquad \phi_c^q = 0 \tag{42}$$

for $j = 1, \ldots, n_\phi$ and $q = 1, \ldots, n_{\phi-1}$. The solution and loading terms p_z^i are expanded in a double Fourier series, satisfying the boundary conditions identically, as

$$(w_0, \phi^j, \phi_c^q, p_z^i) = \sum_{m=1}^{\infty}\sum_{n=1}^{\infty}(w_0, \phi^j, \phi_c^q, p_z^i)_{mn}\sin\bar{m}x\sin\bar{n}y$$
$$(u_{0_x}, u_{1_x}^0, u_{2_x}^0, \psi_{0_x}) = \sum_{m=1}^{\infty}\sum_{n=1}^{\infty}(u_{0_x}, u_{1_x}^0, u_{2_x}^0, \psi_{0_x})_{mn}\cos\bar{m}x\sin\bar{n}y$$
$$(u_{0_y}, u_{1_y}^0, u_{2_y}^0, \psi_{0_y}) = \sum_{m=1}^{\infty}\sum_{n=1}^{\infty}(u_{0_y}, u_{1_y}^0, u_{2_y}^0, \psi_{0_y})_{mn}\sin\bar{m}x\cos\bar{n}y \tag{43}$$

with $\bar{m} = m\pi/a$ and $\bar{n} = n\pi/b$. Substituting these expressions in Eq. (40) yields a system of algebraic equations for the (m, n)th Fourier component:

$$K\bar{U}^{mn} = \bar{P}^{mn} \tag{44}$$

Table 1 Material properties

Property	Units	Material 1	Material 2	Material 3	PZT-5A
Y_1	G · Pa	172.5	224.25	181.0	61.0
Y_2	G · Pa	6.9	6.9	10.3	61.0
Y_3	G · Pa	6.9	6.9	10.3	53.2
G_{12}	G · Pa	3.45	56.58	7.17	22.6
G_{23}	G · Pa	1.38	1.38	2.87	21.1
G_{31}	G · Pa	3.45	56.58	7.17	21.1
ν_{12}	——	0.25	0.25	0.28	0.35
ν_{13}	——	0.25	0.25	0.28	0.38
ν_{23}	——	0.25	0.25	0.33	0.38

$\bar{U}$ is partitioned into U (containing the nine mechanical displacement variables), Φ_s (containing the unknown output voltages at locations $z = z_\phi^j$ where ϕ is not prescribed), and Φ_a (containing the known actuation voltages). $\bar{P}$ is also partitioned accordingly. Equation (44) is then solved for the unknown variables U and Φ_s. All stress components, including transverse shear stresses and the electric displacements, are computed using the constitutive Eqs. (3).

IV. Numerical Results and Discussion

To illustrate the effect of the new local second- and third-order terms introduced in the present theory, results of the present theory are compared with those of the conventional ZIGT [12] for both elastic and hybrid composite plates. Their relative accuracy is ascertained by direct comparison with exact 3-D elasticity [18] and piezoelasticity [4] solutions for simply supported rectangular plates. The mechanical properties of graphite–epoxy composite materials 1, 2, and 3 and the piezoelectric material PZT-5A used in the laminates are given in Table 1, where Y_i, G_{ij}, and ν_{ij} denote Young's moduli, shear moduli, and Poisson's ratios, respectively. The electromechanical properties of PZT-5A are

$$[(d_{31}, d_{32}, d_{33}, d_{15}, d_{24}), (\eta_{11}, \eta_{22}, \eta_{33})] = [(-171, -171, 374, 584, 584)10^{-12}\ \text{m/V}, (1.53, 1.53, 1.5)10^{-8}\ \text{F/m}]$$

A. Elastic Composite Plates in Cylindrical Bending

Simply supported cross-ply composite panels in cylindrical bending made of material 1 are analyzed for sinusoidal pressure $p_z^2 = -p_0 \sin(\pi x/a)$ applied on the top surface. The results are nondimensionalized with $S = a/h$ and $Y_0 = 6.9$ GPa as

$$(\bar{u}, \bar{w}) = (u, w)Y_0/ap_0, \qquad (\bar{\sigma}_x, \bar{\tau}_{zx}) = (\sigma_x, \tau_{zx})/p_0$$

The through-the-thickness distributions of $\bar{u}$ and $\bar{\tau}_{zx}$ at the support ($x = 0$) and $\bar{w}$ and $\bar{\sigma}_x$ at the midspan $x = a/2$ for two-layer (0 deg /90 deg), three-layer (0 deg /90 deg /0 deg), and seven-layer (0 deg /90 deg /0 deg /90 deg /0 deg /90 deg /0 deg)

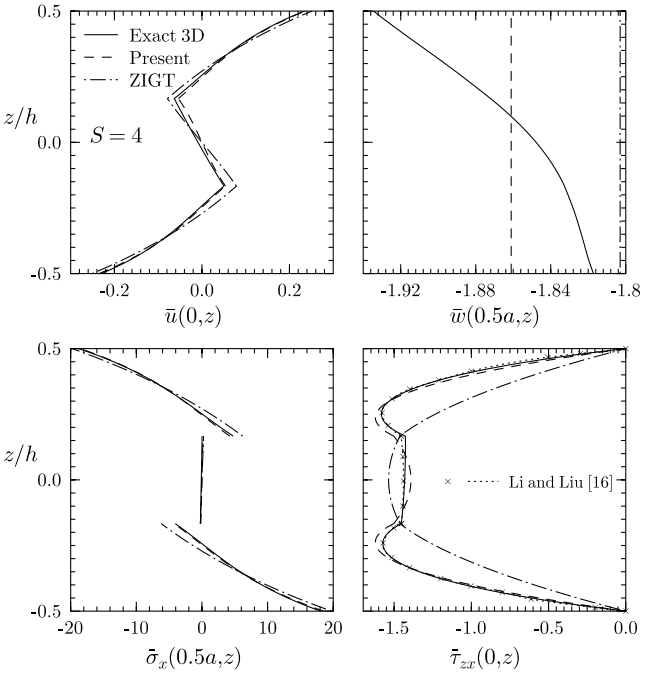

Fig. 3 Through-the-thickness distributions of $\bar{u}$, $\bar{w}$, $\bar{\sigma}_x$, and $\bar{\tau}_{zx}$ for a three-layer composite panel under pressure load.

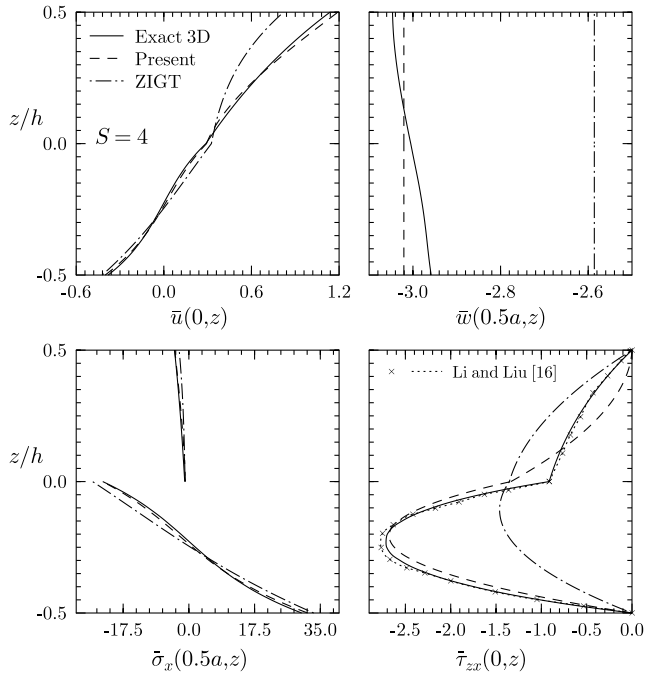

Fig. 2 Through-the-thickness distributions of $\bar{u}$, $\bar{w}$, $\bar{\sigma}_x$, and $\bar{\tau}_{zx}$ for a two-layer composite panel under pressure load.

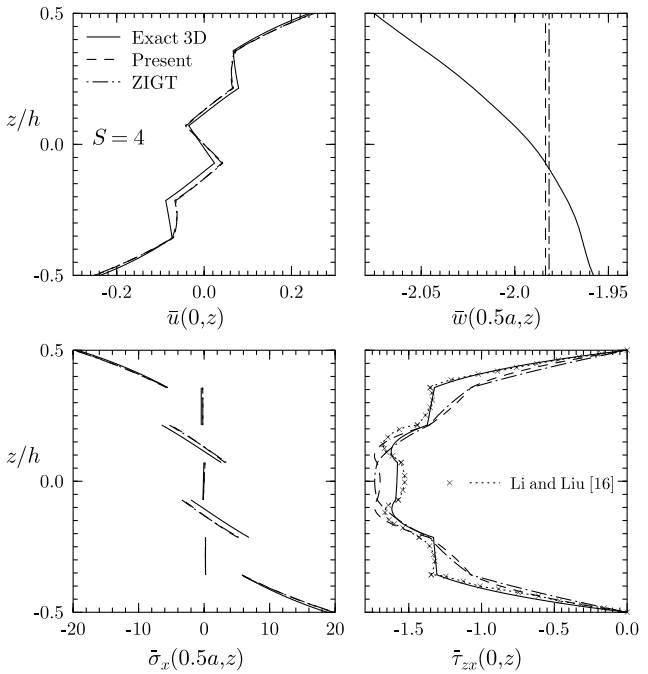

Fig. 4 Through-the-thickness distributions of $\bar{u}$, $\bar{w}$, $\bar{\sigma}_x$, and $\bar{\tau}_{zx}$ for a seven-layer composite panel under pressure load.

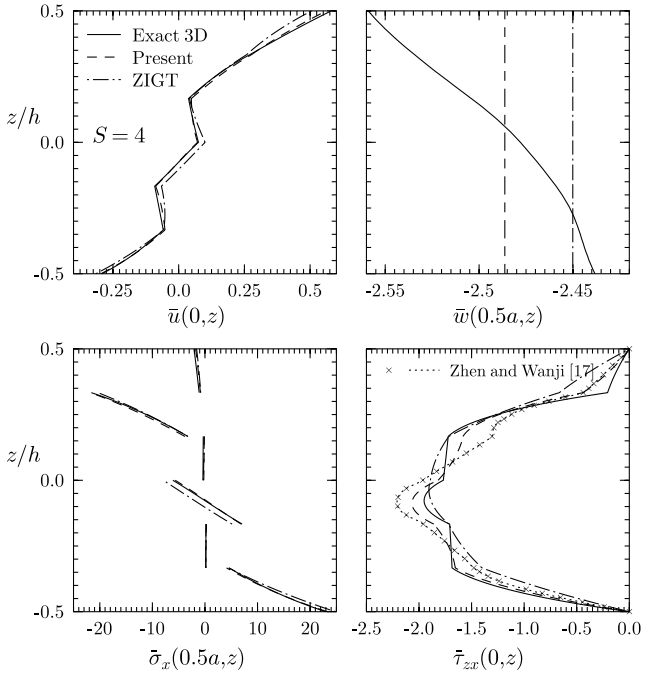

Fig. 5 Through-the-thickness distributions of $\bar{u}$, $\bar{w}$, $\bar{\sigma}_x$, and $\bar{\tau}_{zx}$ for a six-layer antisymmetric composite panel under pressure load.

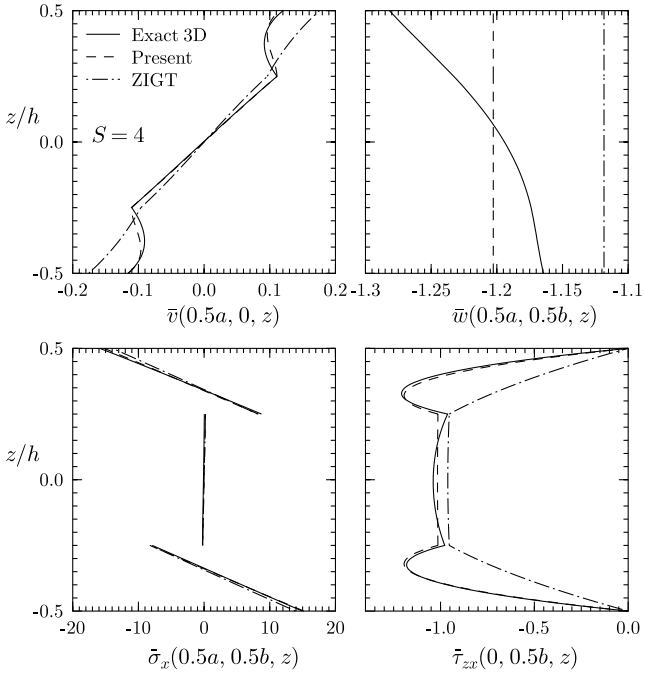

Fig. 6 Through-the-thickness distributions of $\bar{v}$, $\bar{w}$, $\bar{\sigma}_x$, and $\bar{\tau}_{zx}$ for a four-layer composite rectangular plate under pressure load.

symmetric composite panels with $S = 4$ are presented in Figs. 2–4, respectively. The distributions of $\bar{\tau}_{zx}$, based on the 1,2-3 GLT of Li and Liu [16], are also shown for comparison. Similar results for six-layer antisymmetric (0 deg /90 deg /0 deg /90 deg /0 deg / 90 deg) panel with $S = 4$ are presented in Fig. 5 and compared with those of Zhen and Wanji [17] based on the GLT. It is revealed that the present theory yields more accurate distributions than the ZIGT, not only for the transverse shear stress $\bar{\tau}_{zx}$, but also for the in-plane and transverse displacements and in-plane stresses in all cases. For the symmetric laminates, the GLT with 11 primary displacement variables predicts distributions of $\bar{\tau}_{zx}$ more accurately than the present theory with nine unknowns, but the present theory also predicts the maximum value of $\bar{\tau}_{zx}$ quite accurately. For the unsymmetric six-layer laminate, however, the present theory's predictions of $\bar{\tau}_{zx}$ are better than that of the GLT.

B. Rectangular Elastic Composite Plate

An all-around simply supported rectangular composite plate of four-layer (0 deg /90 deg /90 deg /0 deg) symmetric laminate of graphite–epoxy (material 2) is analyzed next for bisinusoidal pressure $p_z^2 = -p_0 \sin(\pi x/a) \sin(\pi y/b)$ applied on the top surface. The results are nondimensionalized, as previously mentioned. The through-the-thickness distributions according to the 3-D elasticity solution, the present theory, and the ZIGT are presented in Fig. 6 for $S = 4$ and $b/a = 2$. It is revealed that the present theory is able to predict the distributions of $\bar{v}$, $\bar{\sigma}_x$, and $\bar{\tau}_{zx}$ very accurately, including the nonlinear variations in $\bar{v}$ and $\bar{\tau}_{zx}$ in the top and bottom layers, which the ZIGT is unable to predict. Even though the nonlinear variation of w is not captured by the 2-D theories with constant w, the central deflection is more accurately predicted by the present theory than the ZIGT.

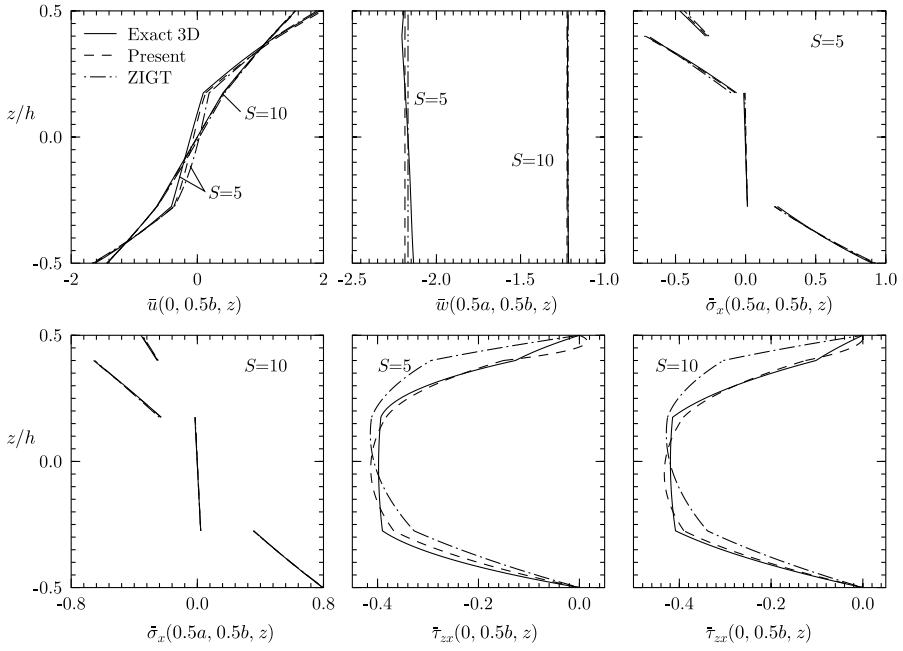

Fig. 7 Through-the-thickness distributions of $\bar{u}$, $\bar{w}$, $\bar{\sigma}_x$, and $\bar{\tau}_{zx}$ for a hybrid composite plate under pressure load.

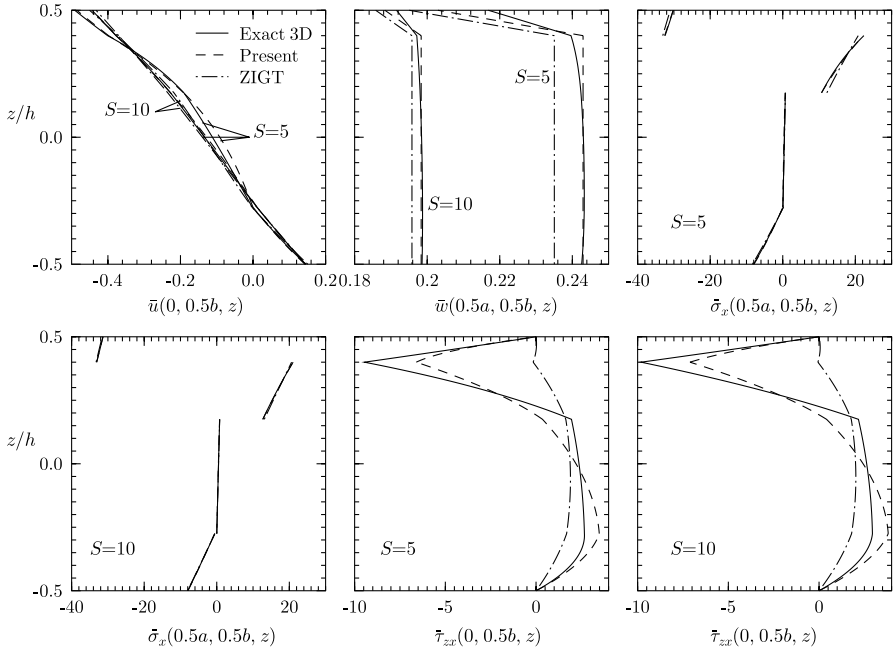

Fig. 8 Through-the-thickness distributions of $\bar{u}$, $\bar{w}$, $\bar{\sigma}_x$, and $\bar{\tau}_{zx}$ for a hybrid composite plate under potential load.

C. Rectangular Hybrid Composite Plate

The rectangular hybrid composite plate with $b/a = 3$ analyzed in [12] is considered next. The plate has a four-layer graphite–epoxy laminate [0 deg /90 deg /90 deg /0 deg] of material 3, with each layer of thickness $0.225h$. A PZT-5A layer of thickness $0.1h$, having poling along the $+z$ direction, is bonded to the top of the elastic laminate called substrate. The interface between the substrate and the piezoelectric layer is grounded. Two load cases are considered as follows:

1) Pressure $p_z^2 = -p_0 \sin(\pi x/a) \sin(\pi y/b)$ is applied on the top surface, which is grounded.

2) Actuation potential $\phi^{n_\phi} = \phi_0 \sin(\pi x/a) \sin(\pi y/b)$ is applied on the top surface.

The results for these two load cases are nondimensionalized with $d_0 = 374 \times 10^{-12}$ CN^{-1} and $Y_0 = 10.3$ GPa as follows:

1) $(\bar{u}, \bar{w}) = 100(u, w/S)Y_0/hS^3 p_0$ and $(\bar{\sigma}_x, \bar{\tau}_{zx}) = (\sigma_x, S\tau_{zx})/S^2 p_0$.

2) $(\bar{u}, \bar{w}) = (u, w/S)/Sd_0\phi_0$ and $(\bar{\sigma}_x, \bar{\tau}_{zx}) = (\sigma_x, S\tau_{zx})h/Y_0 d_0 \phi_0$.

The through-the-thickness distributions of $\bar{u}$, $\bar{w}$, $\bar{\sigma}_x$, and $\bar{\tau}_{zx}$ obtained from the present theory, the ZIGT, and the piezoelasticity solution [4] for thick ($S = 5$) and moderately thick ($S = 10$) hybrid plates are compared in Figs. 7 and 8 for load cases 1 and 2, respectively. It is revealed that, in general, the present theory yields superior results compared with the ZIGT. In particular, $\bar{\tau}_{zx}$ predicted by the ZIGT from direct constitutive relations for potential load case 2 is highly erroneous, whereas the present theory has shown considerable improvement. However, more accuracy is desirable in predicting the transverse shear stress at the interface of actuated piezoelectric layers for reliable results. The improvement in the present theory over the ZIGT for the prediction of transverse displacement w under load case 2 is also very significant.

V. Conclusions

The new coupled local higher-order ZIGT for hybrid piezoelectric plates is a significant improvement over the existing ZIGT, not only in predicting transverse shear stresses directly from constitutive equations without any postprocessing, but also for other stresses and displacements. The inclusion of local higher-order terms in the expression of in-plane displacements enables predictions of higher-order layerwise variations of in-plane displacements as well as transverse shear stresses quite accurately. Of particular significance is the much improved prediction of transverse shear stresses at the interface between the host substrate and the actuated layer directly from constitutive equations, for which the existing ZIGT yields very poor results. The prediction of deflection for the electric potential load case by the present theory is also very accurate and superior to the ZIGT.

References

[1] Chopra, I., "Review of State of Art of Smart Structures and Integrated Systems," *AIAA Journal*, Vol. 40, No. 11, 2002, pp. 2145–2187. doi:10.2514/2.1561

[2] Heyliger, P., "Static Behaviour of Laminated Elastic/Piezoelectric Plates," *AIAA Journal*, Vol. 32, No. 12, 1994, pp. 2481–2484. doi:10.2514/3.12321

[3] Lee, J. S., and Jiang, L. Z., "Exact Electroelastic Analysis of Piezoelectric Laminae Via State Space Approach," *International Journal of Solids and Structures*, Vol. 33, No. 7, 1996, pp. 977–990. doi:10.1016/0020-7683(95)00083-6

[4] Kapuria, S., Dumir, P. C., and Sengupta, S., "Three-Dimensional Solution for Shape Control of a Simply Supported Rectangular Hybrid Plate," *Journal of Thermal Stresses*, Vol. 22, No. 2, 1999, pp. 159–176. doi:10.1080/014957399280940

[5] Heyliger, P. R., Ramirez, G., and Saravanos, D. A., "Coupled Discrete-Layer Finite Elements for Laminated Piezoelectric Plates," *Communications in Numerical Methods in Engineering*, Vol. 10, No. 12, 1994, pp. 971–981. doi:10.1002/cnm.1640101203

[6] Suleman, A., and Venkayya, V. B., "A Simple Finite Element Formulation for a Laminated Composite Plate with Piezoelectric Layers," *Journal of Intelligent Material Systems and Structures*, Vol. 6, No. 6, 1995, pp. 776–782. doi:10.1177/1045389X9500600605

[7] Kapuria, S., and Dumir, P. C., "Coupled FSDT for Piezothermoelastic Hybrid Rectangular Plate," *International Journal of Solids and Structures*, Vol. 37, No. 42, 2000, pp. 6131–6153. doi:10.1016/S0020-7683(99)00248-6

[8] Polit, O., and Bruant, I., "Electric Potential Approximations for an Eight Node Plate Finite Element," *Computers and Structures*, Vol. 84, Nos. 22–23, 2006, pp. 1480–1493. doi:10.1016/j.compstruc.2006.01.032

[9] Mitchell, J. A., and Reddy, J. N., "A Refined Hybrid Plate Theory for Composite Laminates with Piezoelectric Laminae," *International Journal of Solids and Structures*, Vol. 32, No. 16, 1995, pp. 2345–2367. doi:10.1016/0020-7683(94)00229-P

[10] Thornburgh, R. P., Chattopadhyay, A., and Ghosal, A., "Transient Vibration of Smart Structures Using a Coupled Piezoelectric-Mechanical Theory," *Journal of Sound and Vibration*, Vol. 274, Nos. 1–2, 2004, pp. 53–72. doi:10.1016/S0022-460X(03)00648-5

[11] Kapuria, S., and Achary, G. G. S., "A Coupled Consistent Third-Order Theory for Hybrid Piezoelectric Plates," *Composite Structures*, Vol. 70, No. 1, 2005, pp. 120–133. doi:10.1016/j.compstruct.2004.08.018

[12] Kapuria, S., "A Coupled Zig-Zag Third-Order Theory for Piezoelectric Hybrid Cross-Ply Plates," *Journal of Applied Mechanics*, Vol. 71, No. 5, 2004, pp. 604–614. doi:10.1115/1.1767170

[13] Kapuria, S., and Achary, G. G. S., "A Coupled Zigzag Theory for the Dynamics of Piezoelectric Hybrid Cross-Ply Plates," *Archive of Applied Mechanics*, Vol. 75, No. 1, 2005, pp. 42–57. doi:10.1007/s00419-005-0386-5

[14] Cho, M., and Parmerter, R. R., "Efficient Higher Order Composite Plate Theory for General Lamination Configurations," *AIAA Journal*, Vol. 31, No. 7, 1993, pp. 1299–1306. doi:10.2514/3.11767

[15] Shu, X., and Sun, L., "An Improved Simple Higher-Order Theory for Laminated Composite Plates," *Computers and Structures*, Vol. 50, No. 2, 1994, pp. 231–236. doi:10.1016/0045-7949(94)90298-4

[16] Li, X., and Liu, D., "Generalized Laminate Theories Based on Double Superposition Hypothesis." *International Journal for Numerical Methods in Engineering*, Vol. 40, No. 7, 1997, pp. 1197–1212. doi:10.1002/(SICI)1097-0207(19970415)40:7<1197::AID-NME109>3.0.CO;2-B

[17] Zhen, W., and Wanji, C., "A Study of Global–Local Higher-Order Theories for Laminated Composite Plates," *Composite Structures*, Vol. 79, No. 1, 2007, pp. 44–54. doi:10.1016/j.compstruct.2005.11.027

[18] Pagano, N. J., "Exact Solutions for Composite Laminates in Cylindrical Bending," *Journal of Composite Materials*, Vol. 3, No. 3, 1969, pp. 398–411. doi:10.1177/002199836900300304

[19] Auld, B. A., *Acoustic Fields and Waves in Solids*, Vol. 1, Wiley, New York, 1973, p. 373.

[20] Tiersten, H. F., *Linear Piezoelectric Plate Vibrations*, Plenum, New York, 1969, pp. 25, 37, 54, 55.

A. Palazotto
Associate Editor